Comparison of an Adaptive Wavelet Method and Nonlinearly Filtered Pseudospectral Methods for Two-Dimensional Turbulence[1]

K. Schneider

ICT, Universität Karlsruhe (TH),
Kaiserstraße 12, 76128 Karlsruhe, Germany
and
Centre de Physique Théorique, CNRS - Luminy,
Case 907, 13288 Marseille cedex 09, France

N.K.-R. Kevlahan and M. Farge

LMD-CNRS, Ecole Normale Supérieure,
24 rue Lhomond, 75231 Paris cedex 05, France

Abstract. An adaptive wavelet method for solving the two-dimensional Navier–Stokes equations is compared with nonlinear Fourier filtering and nonlinear wavelet filtering of the pseudospectral method at each time step. The methods are each applied to a highly nonlinear flow typical of two-dimensional turbulence, the merger of two positive vortices pushed together by a weaker negative vortex, and the results are compared with a reference classical pseudospectral method. Nonlinear Fourier filtering uses 1.7 times fewer active modes than the reference simulation at the time of merger (when the flow is most complicated) and retains the overall dynamics and structure of the flow. However, it induces spurious oscillations in the background. Nonlinear wavelet filtering simulation uses 9.2 times fewer modes than the reference simulation at the time of merger, and reduces the errors in the solution. The adaptive wavelet simulation replicates precisely the dynamics and spatial structure of the reference simulation while retaining the high compression rate of the nonlinear wavelet filtering simulation. In addition we observe that the number of active wavelet modes remains quasi-constant during the whole merging process, independent of the strength of the vorticity gradients. On the contrary, the number of active Fourier modes is multiplied by 5 when the vorticity gradients are strongest. The increased accuracy of the adaptive wavelet simulation is due to the security zone added around the active coefficients and to the compression of the nonlinear term of the Navier–Stokes equations in the wavelet basis. These results suggest that nonlinear Fourier filtering of a classical pseudospectral method cannot produce significant improvement, but that the adaptive wavelet method combines a consistently high compression rate with high accuracy.

---

1. Introduction

Wavelet methods have been associated with turbulence, almost since their invention, to analyze the structure and dynamics of the flow [12], [14], [16], [30], [13], [15]. These studies have shown that the strongest modes of the wavelet transform of a two-dimensional turbulent flow represent the coherent structures (e.g. vortices), while the weaker modes represent the unorganized background flow. Furthermore, it has been found that the coherent vortices can be well represented by only a very few wavelet modes [44]. These observations suggest that wavelets could be an efficient basis for two-dimensional turbulent flows since the dynamics of such flows are largely controlled by their coherent vortices.

Inspired by these observations, several researchers have begun to develop wavelet-based schemes for actually solving the Navier–Stokes equations that govern two-dimensional turbulence [7], [19], [21]. These schemes take advantage of the compression of both the vorticity field and the operator involved, e.g. , $(I - \Delta t \, \nu \, \partial^2 / \partial x^2)^{-1}$, in the wavelet basis in order to simulate two-dimensional turbulence with a reduced number of active modes. The hope is that wavelet-based simulations will allow higher Reynolds number flows (where the Reynolds number measures the ratio of inertial to viscous forces) to be simulated because the number of modes required should increase more slowly with Reynolds numbers than for the pseudospectral methods currently used. In particular, Kevlahan and Farge [23] have conjectured that the vortex density does not increase with Reynolds number because coherent vortices inhibit the formation of new vortices in their vicinity. If this is indeed the case the advantage of wavelet-based methods should be especially strong at high Reynolds number since the number of wavelet modes required scales roughly with the number of coherent vortices. The simulation of high Reynolds number flows is essential if direct numerical simulations of the Navier–Stokes equations are to be useful for engineering (combustion, aeronautics, . . .) and geophysical applications.

The aim of this paper is to validate such an adaptive wavelet-based numerical method against the classical pseudospectral method for a particular highly nonlinear flow typical of two-dimensional turbulence: the rapid merger of two positive vortices pushed together by a weaker negative vortex. In addition to checking that the adaptive wavelet method reproduces accurately the dynamics and spatial structure of the flow as calculated by the pseudo-spectral method, we also compare it with two nonlinear filtering schemes for the pseudospectral method. The performance of the filtering schemes will give some idea of the potential for improving the efficiency of the pseudospectral method at higher Reynolds numbers.

In the following section we discuss the relative merits of the various numerical methods in use for solving the Navier–Stokes equations and the potential advantages of the adaptive wavelet method. In Section 3 we introduce the equations to be solved and explain the various numerical algorithms used. In Section 4 we present the results of the simulations and these results are discussed and summarized in Section 5.

2. Numerical Methods for Turbulence

In the last 25 years the progress in numerical methods and the availability of supercomputers have had a significant impact on turbulence research. For example, the importance and role of coherent vortices (vortex tubes) in three-dimensional turbulence has been established largely by high resolution numerical simulations [1], [42], [43]. Von Neumann's vision, who had suggested in 1949 [33] that turbulence could be simulated numerically, has become a reality.

However, direct numerical simulations (DNS) of turbulence, which numerically solve the Navier–Stokes equations with no additional turbulence models, are limited to only moderate Reynolds numbers and simple geometries. To approach the Reynolds numbers typical of engineering or geophysical flows the Navier–Stokes equations must still be simplified using some sort of *ad hoc* model to mimic the effect of subgrid scale motions on the resolved motions. Unfortunately, turbulence modeling is still extremely difficult due to our lack of knowledge of the intrinsic dynamics of turbulent flows. Moreover, simulations using turbulence models cannot substantially advance our understanding of turbulence since they only model the flow dynamics statistically (they mimic the subgrid scale dynamics by a stochastic process).

Apart from laboratory experiments, DNS are thus the only numerical methods that can give more reliable information about the dynamics of turbulence. The DNS schemes currently in use may be classified into three categories:

1. Spectral and pseudospectral schemes.
2. Finite-difference, -volume, and -element methods.
3. Lagrangian methods, e.g. vortex methods and contour dynamics.

Note that categories 1 and 2 are both Eulerian methods. The various methods are characterized by differences in their numerical complexity, accuracy, and flexibility.

In DNS the evolution of all scales of the unsteady structures in a turbulent flow field can only be calculated for moderate Reynolds numbers. The severe limit of DNS is that the number of degrees of freedom N for a regular discretization depends on the Reynolds number Re, such that $N \sim Re$ for two-dimensional flows and $N \sim Re^{9/4}$ for the three-dimensional case. Therefore only moderate Reynolds number flows ($Re \sim 10^3$ in three dimensions) can be simulated at present. Although most flows of engineering interest have higher Reynolds numbers ($Re \sim 10^7$), some physical insight can be gained from studying DNS of only moderate Re flows. However, laboratory experiments have shown that new behavior appears in the range $Re \sim 10^4$–10^5, corresponding to the mixing transition [9]. Because of the way the number of degrees of freedom scales with Reynolds number, the simulation of such high Reynolds number flows in two or three dimensions will require schemes employing some sort of adaptive discretization.

DNS are also limited currently to simple boundary conditions. When considering homogeneous isotropic flows periodic boundary conditions can be justified physically in order to achieve maximum symmetry. In this case the Fourier transform-based pseudospectral methods are particularly attractive due to their accurate representation of all flow variables. Once again, however, such highly symmetric and homogeneous turbulent flows are rare in nature and have been selected due to their relative theoretical and numerical simplicity rather than for their physical relevance.

By far the most common type of DNS used in turbulence is the pseudospectral method [6], and most codes are based on the pioneering work of Patterson and Orszag [34] and Rogallo [37]–[39]. Finite-element, -volume, or -difference methods have been far less commonly used, perhaps because they are less precise, less efficient or less optimized for the case of homogeneous flows with periodic boundary conditions (in at least one direction) that are usually investigated. Contour dynamics methods have been extensively used for the simulation of two-dimensional vortex flows [29], [10], but they do not actually solve the Navier–Stokes equations since viscous dissipation is modeled by artificially removing structures thinner than a certain threshold ("contour surgery") and there is no diffusion. Contour dynamics simulations are supposed to simulate extremely high Reynolds numbers, but the question of whether they converge to the $Re \to \infty$ limit of the Navier–Stokes equations is still open.

To our knowledge no current nonwavelet DNS method for incompressible turbulence uses a spatial discretization that adapts to the dynamics and structure of the flow. Adaptive methods, such as shock-capturing, have been developed to treat well-defined features of some flows, but these methods are specialized to specific problems and do not apply to the turbulence itself. In [18] and [21] an adaptive wavelet scheme is proposed for nonlinear PDEs. This method has been recently extended to the two-dimensional Navier–Stokes equations [19], [20] where it has been applied for the simulation of decaying turbulence. Since the wavelet basis functions are localized in both physical and spectral space this approach is a compromise between grid-point methods and spectral methods. The adaptive wavelet method is a good candidate for turbulence simulations because the characteristic structures of turbulence are localized coherent vortices with a multiscale structure [16]. Thus the space- and scale-adaptivity of the wavelet basis should be very efficient at representing turbulence structures and their dynamics.

For simplicity we restrict our attention to two-dimensional flows. The number of degrees of freedom N of a regularly discretized DNS is proportional to the square of the ratio of the largest to smallest scales, which for two-dimensional turbulence is proportional to the Reynolds number Re. Now, pseudo-spectral simulation methods have a computational complexity of $O(N \log_2 N)$, while the adaptive wavelet method has a complexity of only $O(N_c)$ (where N_c denotes the number of the degrees of freedom adapted to the solution, $N_c \leq N$). Note, however, that the actual computational cost depends on the details of the implementation.

As an intermediate step between the classical pseudo-spectral method and the adaptive wavelet method we investigate the effect of compression by nonlinear filtering at each time step. This will allow us to check how many modes can be neglected without destroying the dynamics of the flow. We will also determine whether the pseudospectral method can be significantly improved by such a nonlinear filtering technique.

The various numerical methods are described in more detail in the following section.

3. Numerical Algorithms for the Navier–Stokes Equations

3.1. Physical Problem

A two-dimensional incompressible viscous flow is described by the Navier–Stokes equations. In velocity-vorticity formulation the Navier–Stokes equations with no external force are

$$\partial_t \omega + \mathbf{v} \cdot \nabla \omega = \nu \nabla^2 \omega, \tag{3.1}$$
$$\nabla \cdot \mathbf{v} = 0, \tag{3.2}$$

where the velocity field $\mathbf{v} = (u, v)$, the vorticity $\omega = \nabla \times \mathbf{v}$ and ν is the kinematic viscosity. Note that in two dimensions the vorticity is a pseudoscalar perpendicular to the velocity vector. System (3.1) is completed by appropriate boundary and initial conditions. The domain of the simulation is $\Omega = [0, 2\pi] \times [0, 2\pi]$, i.e. a 2π square box, where periodic boundary conditions are imposed; the initial conditions are discussed in Section 4.1.

The kinetic energy of the system is defined as

$$E(t) = \tfrac{1}{2} \int_\Omega \mathbf{v}^2(\mathbf{x}, t) \, d\mathbf{x}, \tag{3.3}$$

where $\mathbf{x} = (x, y)$, and analogously the enstrophy is

$$Z(t) = \tfrac{1}{2} \int_\Omega \omega^2(\mathbf{x}, t) \, d\mathbf{x}. \tag{3.4}$$

The dissipation of energy and enstrophy are related in the following way:

$$d_t E = -2\nu Z, \qquad d_t Z = -2\nu P \tag{3.5}$$

where

$$P(t) = \tfrac{1}{2} \int_\Omega |\nabla \omega|^2 d\mathbf{x} \tag{3.6}$$

denotes the palinstrophy.

The energy spectrum

$$E(k) = \tfrac{1}{2} \sum_{k-1/2 < |\mathbf{k}| \leq k+1/2} |\hat{\mathbf{v}}(\mathbf{k})|^2, \qquad k \in \mathbf{N}, \tag{3.7}$$

and enstrophy spectrum

$$Z(k) = \tfrac{1}{2} \sum_{k-1/2 < |\mathbf{k}| \leq k+1/2} |\hat{\omega}(\mathbf{k})|^2, \qquad k \in \mathbf{N}, \tag{3.8}$$

are defined using the Fourier transform

$$\hat{f}(\mathbf{k}) = \frac{1}{4\pi^2} \int_\Omega f(\mathbf{x}) \exp(-i\mathbf{k} \cdot \mathbf{x}) \, d\mathbf{x}, \tag{3.9}$$

with $\mathbf{k} = (k_x, k_y)$ and $|\mathbf{k}|^2 = k_x^2 + k_y^2$, and measure the amount of energy or enstrophy in the ring of wave numbers between shell k and shell $k + dk$. The energy and enstrophy spectra are related according to the expression $Z(k) = |\mathbf{k}|^2 E(k)$.

3.2. Time Discretization

DNS typically use semi-implicit time schemes [6]. The linear terms are discretized implicitly to stabilize purely explicit schemes (or to improve the severe stability limits of purely explicit schemes). For spectral

methods this is quite cheap as no linear system has to be solved. An explicit discretization of the nonlinear terms avoids the solution of nonlinear equations, however it implies a CFL condition on the maximum size of the time step. The most commonly used schemes are exact integration (often called the technique of integrating factors) for the linear terms or higher order backward differencing formulas. For the nonlinear term Runge–Kutta, Leapfrog, or Adams–Bashforth schemes are usually employed.

The time discretization used for all algorithms discussed in this paper is such a semi-implicit second-order finite difference scheme composed of an Euler backward step for the viscous term and an Adams–Bashforth extrapolation for the convection term. The time discretization of the Navier–Stokes equations (3.1) is thus

$$(\gamma - \nu\nabla^2)\omega^{n+1} = \tfrac{4}{3}\gamma\omega^n - \tfrac{1}{3}\gamma\omega^{n-1} - \mathbf{v}^* \cdot \nabla\omega^*, \tag{3.10}$$

where $\gamma = 3/(2\Delta t)$, $\mathbf{v}^* = 2\mathbf{v}^n - \mathbf{v}^{n-1}$ and $\omega^* = 2\omega^n - \omega^{n-1}$. For start-up a similar first-order scheme is used.

3.3. Pseudospectral Method

Pseudospectral space discretization is the classical method used for DNS of turbulence at small to moderate Reynolds number in two and three dimensions, see [6] for a more complete discussion. It is highly accurate for flows with periodic boundary conditions and will serve as the reference for the other algorithms we consider. In the pseudospectral method the vorticity field is transformed to Fourier space in order to calculate spatial derivatives and evolve the vorticity field in time, but terms containing products are calculated in physical space.

The vorticity field and the other variables are represented as Fourier series, e.g.

$$\omega(\mathbf{x}) = \sum_{\mathbf{k}\in\mathbf{Z}^2} \widehat{\omega}(\mathbf{k})e^{i\mathbf{k}\cdot\mathbf{x}}, \tag{3.11}$$

where $\widehat{\omega}(\mathbf{k})$ is defined in (3.9). The Fourier spatial discretization is thus uniform in space and is truncated at $k = -N/2$ and $k = N/2 + 1$. The gradient of ω is computed by multiplication by $i\mathbf{k}$, the Laplacian by multiplication with $|\mathbf{k}|^2$. The velocity $\mathbf{v}$ is computed using the definition of vorticity in Fourier space, and the incompressibility of the flow in Fourier space, from the relation [28]

$$\mathbf{v}(\mathbf{x}) = \sum_{|\mathbf{k}|\leq N/2,|\mathbf{k}|^2\neq 0} \frac{(-k_y, k_x)}{|\mathbf{k}|^2} \widehat{\omega}(\mathbf{k})e^{i\mathbf{k}\cdot\mathbf{x}}. \tag{3.12}$$

The convection term $\mathbf{v} \cdot \nabla\omega$ is then evaluated by the pseudospectral technique using collocation in physical space without de-aliasing. We do not employ de-aliasing because the simulation is unforced and thus the energy is unlikely to exceed significantly the available range of length-scales. This was checked during the simulation.

3.4. Filtered Spectral Methods

In order to investigate the potential for improving the efficiency of the pseudo-spectral method at higher Reynolds numbers we nonlinearly filter the vorticity field at each time step (which produces a compressed vorticity field), and advance in time classically using the pseudospectral method. This procedure is motivated by the work performed in [13], where such a compression was performed at one time-step, and subsequently the evolution of the compressed vorticity field was calculated. from the physical point of view this calculation may be interpreted as a way of determining the minimal number of degrees of freedom which are required to represent the flow in a particular basis for a given precision. The two types of filtering are described below and the results will be compared with those obtained using the full adaptive wavelet method. Nonlinear filtering means that the filtering process depends on the actual flow. Thus nonlinear filtering is effectively a kind of artificial conditional dissipation.

We choose to filter the vorticity field, rather than the velocity field, because vorticity is highly concentrated into coherent vortices (vorticity is approximately compactly distributed), whereas velocity is spread over all

space. This is reflected in (3.12), where a nonlocal operator, e.g. , $(\nabla^2)^{-1}$, has to be applied to the vorticity in order to calculate the velocity, e.g. the velocity field of a point vortex decays only like $1/r$, where r denotes the distance from its center. The difference in the spatial distribution of vorticity and velocity is generic, and is one of the reasons vorticity is much simpler to deal with in fluid dynamics. In addition, vorticity is a Lagrangian invariant of Euler flow.

3.4.1. Nonlinear Fourier Filtering.   The principle of nonlinear filtering is as follows: at each time-step all Fourier modes of the vorticity field with absolute magnitude below a certain threshold ε are eliminated. Thus this method is adaptive and should adjust to the changing dynamics and structure of the flow. In this approach the choice of the threshold is critical; if it is too large too much energy is lost and the dynamics of the flow are destroyed.

From Parseval's relation the total enstrophy or energy (using 3.12) can be directly expressed in Fourier space as

$$Z = 4\pi^2 \sum_{\mathbf{k}} |\hat{\omega}(\mathbf{k})|^2, \tag{3.13}$$

so that an upper bound for the error in the enstrophy due to the filtering at each time step is given by εN_c where N_c denotes the number of Fourier modes with absolute value below ε.

3.4.2. Nonlinear Wavelet Filtering.   As mentioned in the introduction, wavelets have been found to compress turbulent flows very efficiently. This observation suggests that wavelets might be a good choice for performing efficient nonlinear filtering.

We employ a periodic two-dimensional multiresolution analysis (MRA) [31], [11] and develop ω^n at each time-step n as an orthonormal wavelet series from the largest scale $l_{\max} = 2^0$ to the smallest scale $l_{\min} = 2^J$:

$$\omega^n(x,y) \;=\; c^n_{0,0,0}\varphi_{0,0,0}(x,y) \;\;+\;\; \sum_{j=0}^{J-1} \sum_{i_x=0}^{2^j-1} \sum_{i_y=0}^{2^j-1} \sum_{\mu=1}^{3} d^{\mu,n}_{j,i_x,i_y} \psi^{\mu}_{j,i_x,i_y}(x,y), \tag{3.14}$$

with

$$\varphi_{j,i_x,i_y}(x,y) \;=\; \varphi_{j,i_x}(x)\, \varphi_{j,i_y}(y), \tag{3.15}$$

and

$$\psi^{\mu}_{j,i_x,i_y}(x,y) \;=\; \begin{cases} \psi_{j,i_x}(x)\,\varphi_{j,i_y}(y); & \mu = 1, \\ \varphi_{j,i_x}(x)\,\psi_{j,i_y}(y); & \mu = 2, \\ \psi_{j,i_x}(x)\,\psi_{j,i_y}(y); & \mu = 3, \end{cases} \tag{3.16}$$

where $\varphi_{j,i}$ and $\psi_{j,i}$ are the 2π-periodic one-dimensional scaling function and the corresponding wavelet, respectively.

The modes are given by $c^n_{0,0,0} = \langle \omega^n\,,\,\varphi_{0,0,0}\rangle$ and $d^{\mu,n}_{j,i_x,i_y} = \langle \omega^n\,,\,\psi^{\mu}_{j,i_x,i_y}\rangle$ where $\langle\cdot,\cdot\rangle$ denotes the inner product.

The coefficients are calculated by the fast periodic wavelet transform of [35] using down-sampling in Fourier space [17]. A collocation projection employing an interpolation filter [35] permits an efficient transformation between grid point values $\omega(i_x 2^{-J}, i_y 2^{-J})$ and wavelet coefficients. The complexity of the decomposition and reconstruction algorithms is of the same order as the fast Fourier transform (FFT). In all the following calculations cubic spline wavelets of Battle–Lemarié type have been used. Analytical expressions in Fourier space for the functions and the filters involved can be found in [35] and [17].

At each time step a nonlinear wavelet thresholding technique is performed, i.e. wavelet modes $d^{\mu,n}_{j,i_x,i_y}$ with absolute magnitude below a certain threshold ε are eliminated. Since we have shown [13] that the strong wavelet modes seem to correspond to the coherent structures of the flow and the weak ones to the passively advected background flow, this filtering retains only the coherent vortices and discards the background.

Furthermore, the orthogonality of the wavelets implies that a Parseval relation also holds for the wavelet-filtered flow, i.e.

$$Z = |c_{0,0,0}|^2 \;+\; \sum_{j=0}^{J-1} \sum_{i_x=0}^{2^j-1} \sum_{i_y=0}^{2^j-1} \sum_{\mu=1}^{3} |d^{\mu}_{j,i_x,i_y}|^2, \tag{3.17}$$

and therefore the error in the enstrophy due to filtering can be estimated as in the Fourier case.

3.5. Adaptive Pseudowavelet Method

We use the adaptive wavelet-vaguelette algorithm introduced in [21] and based on the method of [26] which is a pseudowavelet scheme for the solution of nonlinear PDEs. In this method the vorticity is decomposed onto a lacunary basis of orthogonal wavelets. Adaptivity means that the simulation uses only the minimum number of wavelet modes necessary to represent the vorticity field at any given time and position (up to a specified precision ε). As suggested by the nonlinear wavelet-filtered pseudospectral method, we now use the reduced set of wavelet basis functions to compute directly the evolution of the flow.

Expanding the vorticity in an orthogonal wavelet series (3.14) and applying a Petrov–Galerkin scheme to (3.10) with test-functions

$$\theta^{\mu}_{j,i_x,i_y}(x,y) = (\gamma - \nu\nabla^2)^{-1}\,\psi^{\mu}_{j,i_x,i_y}(x,y) \tag{3.18}$$

avoids assembling and solution of a linear system in each time step [26]. The vaguelettes defined in (3.18) can be calculated explicitly in Fourier space and have localization properties similar to those of wavelets [31], [21], i.e. in the case of spline wavelets they have exponential decay. The solution of (3.10) then reduces to the calculation of the coefficients

$$
\begin{aligned}
d^{\mu,n+1}_{j,i_x,i_y} &= \langle \omega^{n+1}, \psi^{\mu}_{j,i_x,i_y}\rangle \\
&= \langle \tfrac{4}{3}\gamma\omega^n - \tfrac{1}{3}\gamma\omega^{n-1}, \theta^{\mu}_{j,i_x,i_y}\rangle - \langle \mathbf{v}^* \cdot \nabla\omega^*, \theta^{\mu}_{j,i_x,i_y}\rangle
\end{aligned}
\tag{3.19}
$$

using an adaptive two-dimensional vaguelette decomposition [4], i.e. only coefficients $d^{\mu,n+1}_{j,i_x,i_y}$ are calculated, which are expected to be larger than ε. The pyramidal decomposition algorithm is based on a subtraction strategy on hierarchical nested grids using the cardinal Lagrange function of the operator-adapted multiresolution analysis [21]. Subsequently, the vorticity field is reconstructed using an adaptive wavelet reconstruction [4], [21]. The nonlinear term is evaluated by a pseudowavelet technique, i.e. , by collocation in physical space. For implementational reasons we currently use a regular grid to evaluate the nonlinear term. A fully adaptive calculation of the nonlinear term is being developed.

If the smoothness of ω varies strongly in space and time it is appropriate to use an adaptive spatial discretization that is recalculated at each time-step. Adaptivity is also important in order to follow the vortices (or other flow structures) as they move about. For the wavelet discretization used here this is accomplished by restricting the full index set

$$\Lambda_J = \left\{(j, i_x, i_y, \mu) | (j = 0,\ldots,J-1), (i_x = 0,\ldots,2^j-1), (i_y = 0, 2^j - 1), (\mu = 1,2,3)\right\} \tag{3.20}$$

to some subset $\Lambda_c \subset \Lambda_J$ depending on the required tolerance ε. The elements designated by Λ_c are termed the "lacunary basis." One is then interested in retaining only those modes with $|d^{\mu}_{j,i_x,i_y}| > \varepsilon$. Orthogonality of the basis and strong decay of the coefficients immediately relates this to the L^2 approximation error, which can therefore be evaluated.

The adaptive algorithm then operates as follows: from the previous time-step those indices with modes larger than the threshold ε are determined. A "security zone" to allow for the evolution of the solution in time is then created by adding to each index of this set its neighboring indices in wavelet space. The solution is then advanced in time by first performing a backward transform of the old solution onto the locally refined grid of quadrature points (this minimizes energy loss due to regridding). The right-hand side is then evaluated at these points. Finally, decomposition onto the operator-adapted basis is applied to determine the new wavelet amplitudes. Thus the adaptive algorithm calculates only at those wavelet modes that are active (plus a securityzone), while the backward transform ensures that the energy of the neglected modes is reinjected back onto the locally refined grid. Recall that in the backward transform all wavelet coefficients which have been calculated are evaluated, so that no coefficients are set to zero. Only then is the reduction of the index set performed.

The magnitude of the threshold parameter ε is crucial to this algorithm, but it cannot at present be determined *a priori*. Ideally, the threshold parameter should be chosen automatically based on the dynamics of the flow, but it is currently not clear how this could be done.

Finally, we mention that the complexity of the algorithm is $O(N_c)$, where N_c denotes the number of wavelet coefficients which are calculated.

Note that a different pseudowavelet method for the Navier–Stokes equations has been recently introduced by Charton and Perrier [7]. They employ an algebraic wavelet method starting with a finite difference scheme on a regular Cartesian grid. Wavelets are then used to speed up the solution procedure by compression of the discrete inverse operator and the actual solution during the time advancement. Furthermore, operator splitting by means of an ADI (alternating direction implicit) technique is applied. The two-dimensional wavelet basis they use relies on a tensor product of two one-dimensional multiresolution analyses. Charton and Perrier [7] apply their method to the three vortex interaction we consider below, and find good qualitative agreement with a reference pseudospectral simulation.

4. Results

4.1. Initial Condition

The initial condition for all simulations considered is

$$\omega(x, y) = \sum_{i=1}^{3} A_i \exp(-((x - x_i)^2 + (y - y_i)^2)/\sigma_i^2) \qquad (4.1)$$

with variance $\sigma_i = 1/\pi$, amplitudes $A_1 = A_2 = -2A_3 = \pi$, and positions $x_1 = 3\pi/4$, $x_2 = x_3 = 5\pi/4$, $y_1 = y_2 = \pi$, $y_3 = \pi(1 + 1/(2\sigma_2))$. This initial condition corresponds to two identical positive Gaussian vortices and one weaker negative Gaussian vortex. Inviscid point vortices in this arrangement collapse to the same point in a finite time $3/8\pi^3\sqrt{2}$ [28] and thus this arrangement ensures a rapid merger corresponding to a highly nonlinear interaction.

These initial conditions are quite specific, but the general dynamics of the vortex merger should not depend critically on the precise arrangement of the vortices. In fully developed two-dimensional turbulent flows the chance of vortex merging increases with the density of vortices. Here with only three vortices we need this specific configuration to ensure a rapid merger; the negative vortex effectively replaces the mean field which pushes vortices together and induces merging. In fact the configuration we have chosen should be fairly realistic since in practice mergers are often caused by a fast-moving dipole running into another vortex: this is modeled by the three vortex initial condition.

The maximal scale J in (3.14) is 8 which corresponds to a maximum of $256 \times 256 = 65,536$ degrees of freedom. Further parameters are $\Delta t = 2.5 \times 10^{-3}$, $\nu = 5 \times 10^{-5}$. The turnover time of one of the positive vortices is initially $T = 4.0$, and the initial Reynolds number based on the circulation of one of the positive vortices is $Re = 2 \times 10^4$. Note that since there is no external forcing the energy and enstrophy decay monotonically in time. By trial and error we determined that the magnitude $\varepsilon = 10^{-6}$ gives satisfactory results. If too large a value of the threshold is used, e.g. , $\varepsilon = 10^{-5}$ (results not shown here), the dynamics of the flow is destroyed: the compression is too strong and the solution differs significantly from the reference method. This result shows that the method is quite sensitive to the size of ε.

The vorticity field, energy and enstrophy spectra, and wavelet modes corresponding to the initial conditions are shown in Figures 1(a), 3(a), and 7(a) respectively. It is interesting to note that nonlinear filtering shows that only 3% of the modes are active at $t = 0$. This is because the solution is initially arbitrarily smooth (which means only a small number of Fourier modes are required) and is also well localized in wavelet space (see Figure 7a).

4.2. Time Evolution of Solutions

The evolution of the vorticity field for each of the four simulation methods is shown in Figure 1. Much fine filamentary structure forms as the two positive vortices wrap around each other and merge to create a new vortex of roughly the same size as one of the original positive vortices [23]. This type of merging interaction is typical of two-dimensional turbulence.

Comparing the four simulations, one notices that the nonlinear Fourier filtering deforms the edge of the vortices and produces spurious oscillations that quickly spread to fill the whole background flow. The error in representing the edges of the vortices is due to the poor ability of Fourier methods to represent
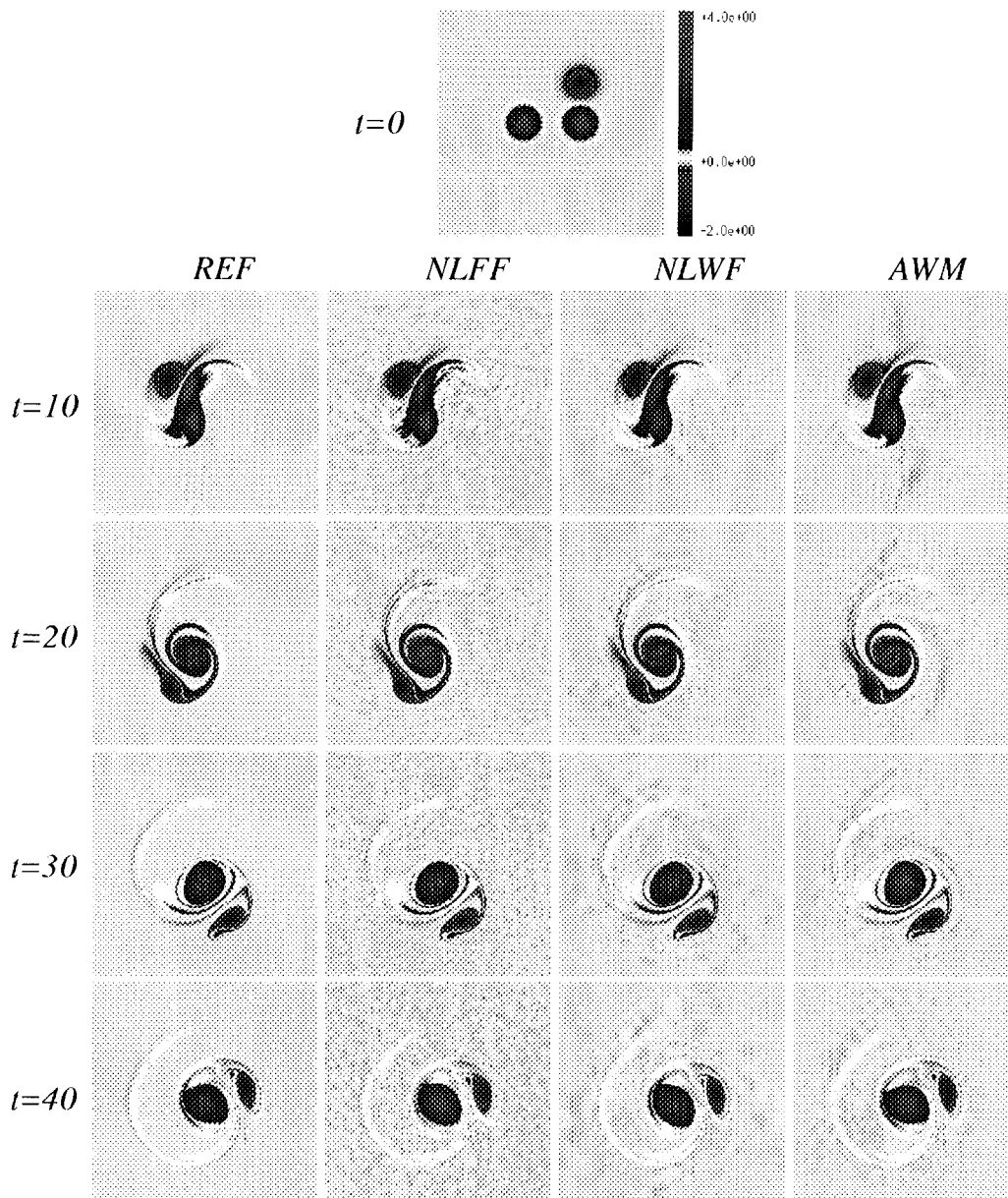
Figure 1. Evolution of the vorticity field as a function of time for each of the four methods. (REF = pseudospectral reference simulation, NLFF = nonlinear Fourier filtering, NLWF = nonlinear wavelet filtering, AWM = adaptive wavelet method.)

localized sharp gradients; this is exacerbated by the filtering. The homogeneous distribution of the error is not surprising since each Fourier mode is completely delocalized in physical space and thus any error is immediately spread over all space.

The nonlinear wavelet filtering simulation is largely free of spurious background oscillations and deformations of the edge of the vortices. However, an error in the phase and orientation of the positive vortex at time $t = 40$ can be clearly seen.

The adaptive wavelet simulation exhibits some slight aliasing problems at $t = 10$, but these quickly disappear. This simulation reproduces the vorticity field of the reference pseudospectral simulation very precisely. If we compare the fields for the four simulations at $t = 40$ we observe that only the adaptive wavelet simulation correctly reproduces the shape and orientation of the positive vortex.
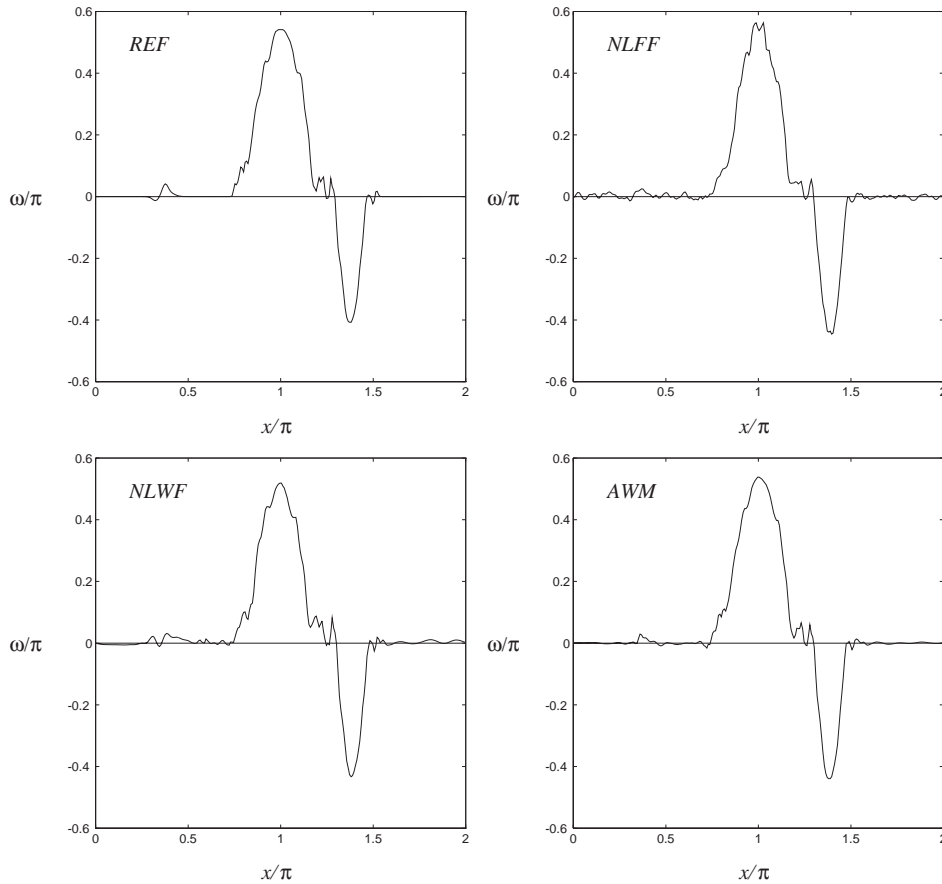
Figure 2. Cut through the vorticity field at position $y = \pi$ and time $t = 40$. Note the spurious oscillations in NLFF, and the fact that AWM matches REF most closely.

Cuts through the vorticity field at $t = 40$ are shown in Figure 2. These cuts allow a more quantitative comparison of the four simulations and confirm the observation that the adaptive wavelet method is closest to the reference simulation. The spurious oscillations induced in the vorticity field and the displacement of the filaments (kinks) by the nonlinear Fourier filtering method show up clearly in Figure 2.

The evolution of the Fourier energy spectra of the four simulations is shown in Figure 3. Note that the energy spectrum is initially Gaussian (it has no power law range), but later fills out and exhibits a power law scaling of roughly $k^{-3.5}$ (close to k^{-3} predicted by Batchelor [3]) in the range $k = (10, 50)$. All simulations produce energy spectra that are very similar to the reference simulation, the only exception being a slight excess of energy at the small scales in the case of nonlinear Fourier filtering. This result shows that the wavelet methods retain the correct spectral structure of the flow. It is not surprising that the nonlinear Fourier filtering method does quite well since it is a Fourier space-based method and we are measuring a Fourier space quantity.

The fact that the energy spectra are very similar for all simulations, even though the physical space structure differs significantly, suggests that it is not a sensitive enough way of comparing different methods for the Navier–Stokes equations. For fully turbulent flows statistical methods based on the relative positions, sizes and shapes of vortices are probably more useful [5], [27]. Recently, Siegel and Weiss [41] have developed a wavelet-packet based algorithm to perform such a "vortex census."

Figure 4 shows that the total energy decreases very slowly and almost linearly with time (losing about 2% of initial energy by $t = 40$), while the enstrophy decreases very rapidly around t, and more slowly at earlier and later times (losing about 30% of initial enstrophy by $t = 40$). The rapid decrease in enstrophy around t is due to the fact that at the time of merging vorticity is pulled out into filaments with high gradients which decay very quickly.
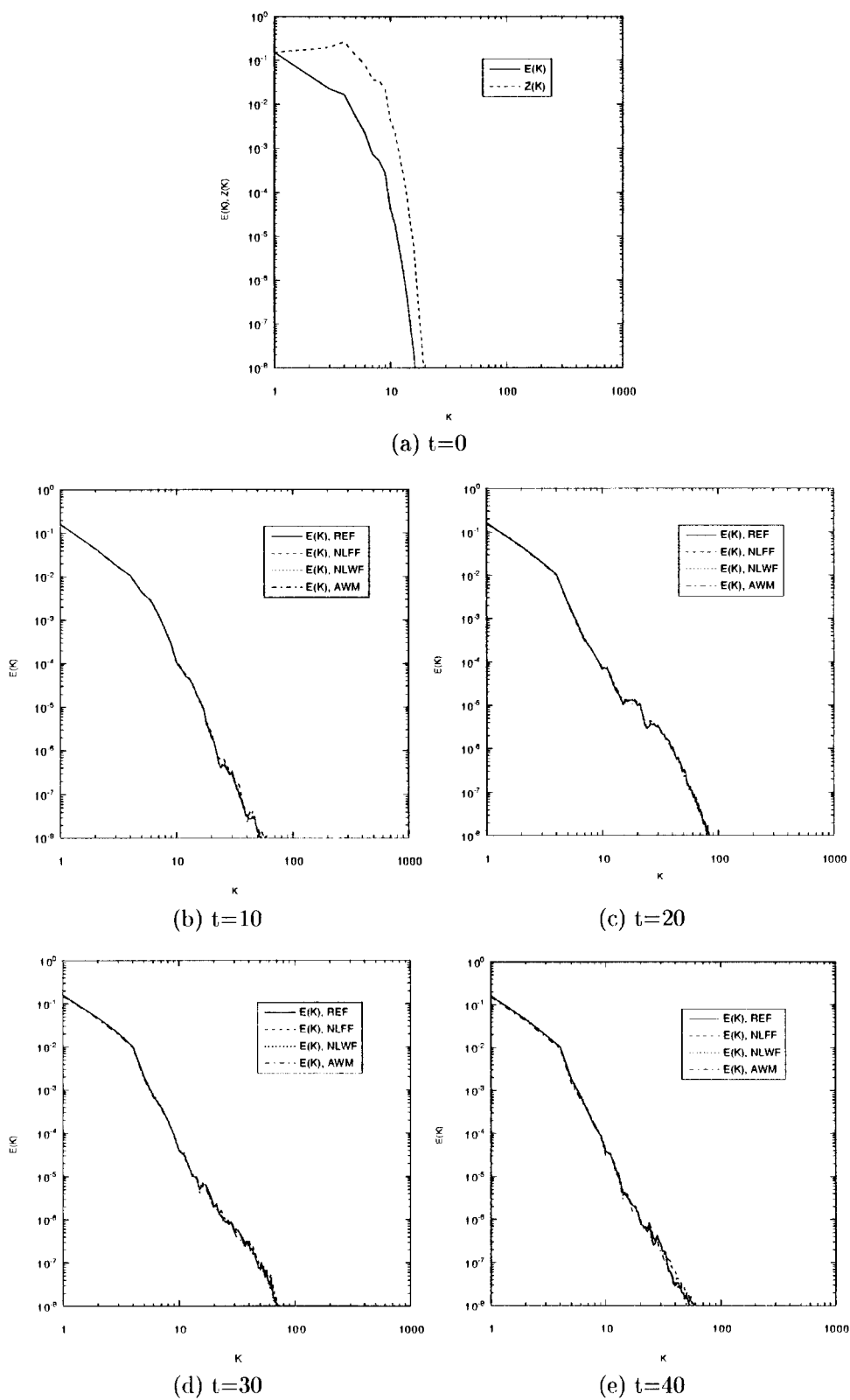
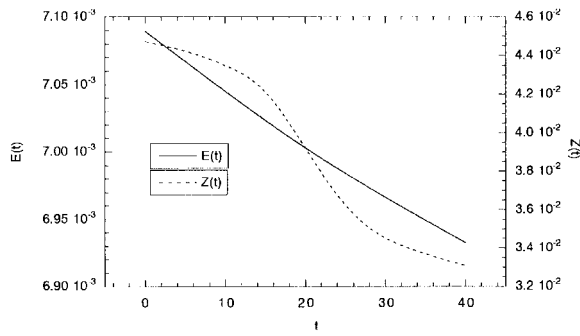**Figure 3.** Evolution of the energy spectrum for the four methods.

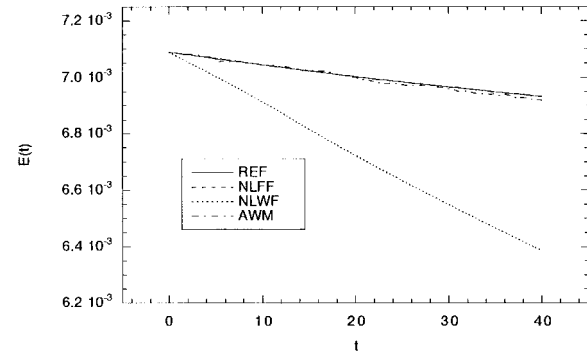**Figure 4.** Evolution of energy and enstrophy in the pseudospectral method.

Figure 5. Comparison of the evolution of energy for the four methods.

The evolution of total energy for the four simulations is compared in Figure 5. The nonlinear wavelet filtering energy has the greatest error, which increases linearly in time (since energy is lost constantly due to the compression). The adaptive wavelet simulation has a fairly small error which does not grow monotonically in time (since the energy of the weak modes is re-injected into the active modes). The nonlinear Fourier filtering exhibits the smallest error in energy. Another reason for the large departure from the reference of the energy of the nonlinear wavelet filtering is the fact that the filtering operates on the vorticity in wavelet space and thus does not necessarily minimize the error in the energy (associated with velocity). The fact that the adaptive wavelet simulation remains close to the reference simulation suggests that the re-injection of enstrophy overcomes this problem. Nevertheless, it is interesting that nonlinear wavelet filtering simulation remains closer to the reference simulation than the nonlinear Fourier filtering simulation despite losing much more energy. This suggests that the energy lost by the nonlinear wavelet filtering is not in fact dynamically important, while the small amount of energy lost by nonlinear Fourier filtering significantly alters the dynamics. This result can be understood physically by noting that the strong wavelet modes correspond to the coherent vortices, which control the flow dynamics, while the weak wavelet modes correspond to the dynamically passive background flow. On the other hand, filtering in Fourier space affects both dynamically active and inactive regions energy because energy is removed evenly over all space.

Figure 7 shows the evolution of wavelet modes as a function of time for the adaptive wavelet simulation. The wavelet coefficients are placed as shown schematically in Figure 6. Note that Figure 7 shows clearly
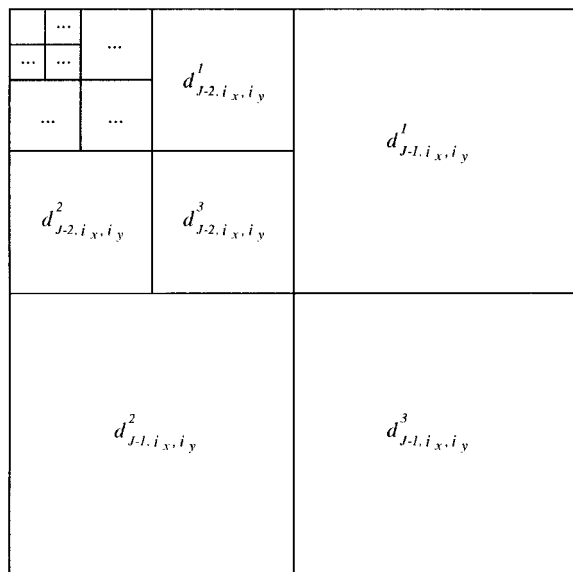

Figure 6. Schematic diagram showing how the wavelet coefficients for a two-dimensional multiresolution analysis are represented (see p. 315 of [8]). The lines separate regions with different j (scale) and different μ (direction). The coefficient d^{μ}_{j,i_x,i_y} gives the magnitude of oscillation of ω with frequency $\xi = 2^j$ near the point $(i_x/2^j, j_y/2^j)$ in the horizontal, vertical or diagonal direction ($\mu = 1, 2, 3$, respectively).
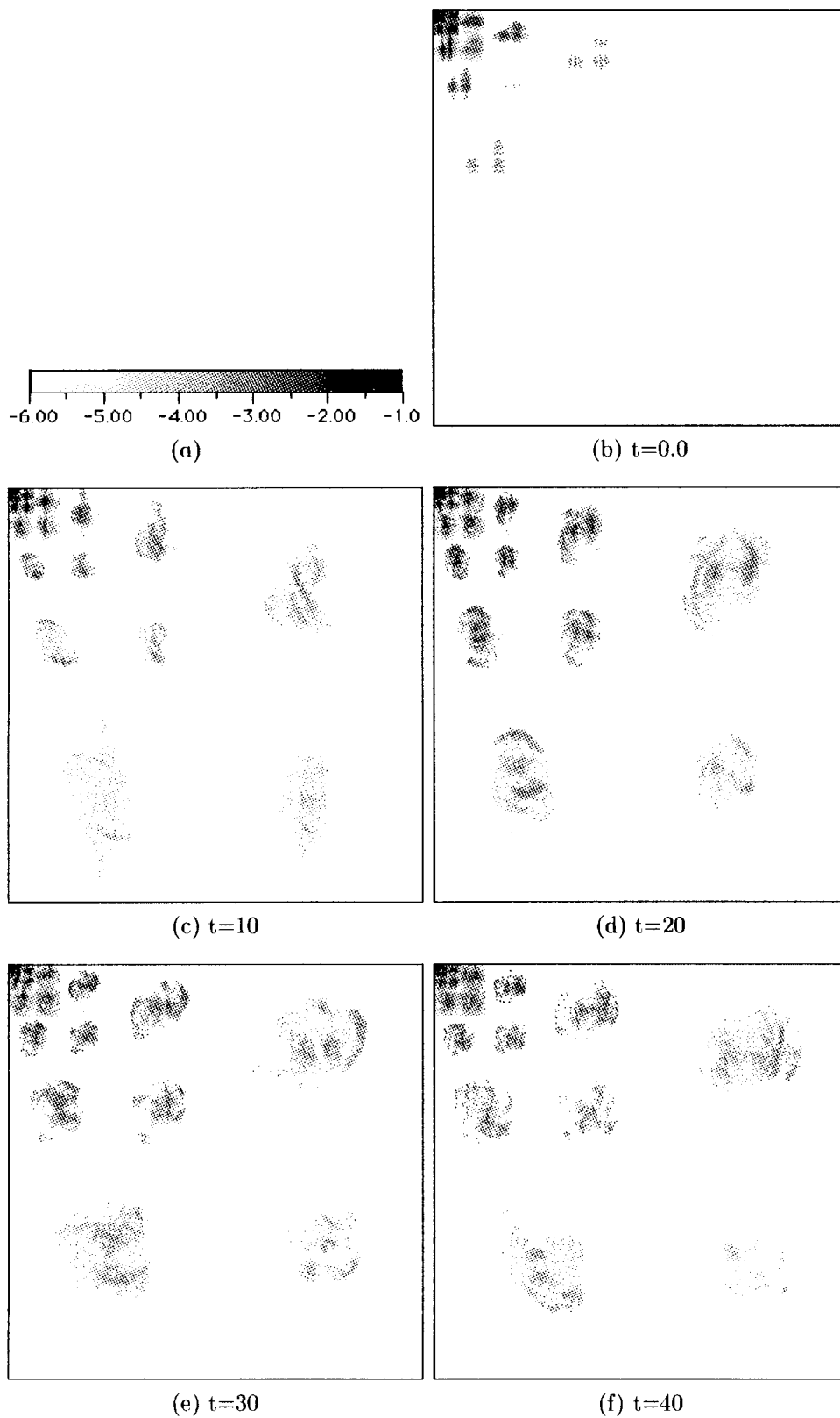
Figure 7. Evolution of wavelet modes for the adaptive wavelet method (darker points are most active). Note that the palette has a logarithmic scale.
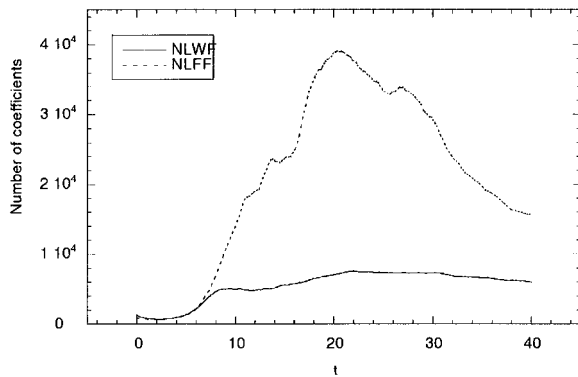
Figure 8. Evolution of the number of active modes for NLFF and NLWF.

how the active modes evolve dynamically in space and scale so as to follow closely the changing shapes of the vortices. This diagram provides a good illustration of the adaptivity of the wavelet algorithm and of its suitability for flows containing coherent structures.

The change in the number of active modes as a function of time for the nonlinear Fourier filtering and wavelet methods is shown in Figure 8. The adaptive wavelet simulation uses 9.2 fewer modes than the reference pseudo-spectral simulation at the time of merging t (when the flow is the most complicated and in strong interaction). It is clear that the nonlinear Fourier filtering method is much less efficient than the wavelet methods and always requires many more modes, except at the start of the simulation. The difference is greatest at about $t = 20$ when 5.5 times more modes are required for nonlinear Fourier filtering. The fact that there is no large peak in the number of wavelet modes at the time of merging (when the structure of the flow is most complex and the gradients of vorticity are the strongest) shows that the wavelet method is very efficient at representing the strong nonlinear interactions (and associated strong gradients of vorticity) that characterize the dynamics of turbulence. This is because the nonlinear interactions are highly localized in physical space which implies delocalization in spectral space, and hence the need for a larger number of Fourier modes to represent the flow.

5. Conclusions

The vortex merging interaction was chosen because it is the strongest nonlinear interaction typical of two-dimensional turbulence. Thus if the adaptive wavelet simulation performs well in this case it should also perform well for a full two-dimensional turbulent flow, which has been demonstrated in [20]. Indeed, the results obtained here show that the number of active wavelet modes remains low even during the most intense phase of the interaction (when the two positive vortices actually merge). The investigation of the two filtering methods (nonlinear Fourier and nonlinear wavelet) suggests that the classical pseudospectral method cannot be made much more efficient using an adaptive nonlinear Fourier filtering method, but that wavelet filtering can produce very high compression rates. It is therefore more attractive to perform the entire simulation in the wavelet basis and, as we note above, the results are promising.

We have shown that the adaptive wavelet simulation is able to reproduce very accurately the dynamics and vorticity structure of a classic pseudospectral simulation of a highly nonlinear interaction of three vortices in two dimensions. In addition, the wavelet simulation uses 9.2 times fewer modes than the pseudospectral simulation at the time of merging (when the flow is most complicated), and retains a consistently high compression rate throughout the simulation. This consistently high compression rate demonstrates the efficiency of wavelets for representing highly nonlinear flows with strong gradients.

Nonlinear Fourier filtering of the pseudospectral simulation uses 5.5 times as many modes as the adaptive wavelet simulation at the time of merging and, while it reproduces the overall dynamics, it introduces spurious oscillations spread over the entire flow.

Nonlinear wavelet filtering, on the other hand, produces fewer, well-localized errors, but loses a significant amount of energy and does not reproduce the structure of the flow as accurately as the adaptive wavelet simulation. The greater accuracy and reduced number of degrees of freedom of the adaptive wavelet

simulation compared with nonlinear wavelet filtering is due to the security zone added around the active coefficients, and to the compression of the nonlinear term of the Navier–Stokes equations in the wavelet basis.

Although the number of modes required in the adaptive wavelet simulation is much less than in the classical pseudospectral simulation, the total calculation time of the former is actually greater (by roughly an order of magnitude). This is due to the fact that the adaptive wavelet code is not yet optimized, and it is likely that significant improvements to the algorithm can be made easily. In principle the adaptive wavelet method has a computational complexity of $O(N_c)$, where N_c ($\leq N$) denotes the number of the degrees of freedom adapted to the solution. The pseudospectral methods, by comparison, are more complex: $O(N \log_2 N)$ where N denotes the number of degrees of freedom on the regular grid. However, the actual numerical cost depends directly on the constant multiplying the order term (which itself depends on the length of the discrete filter and on the various linear operations performed during the computation). At the moment this factor is rather high for the adaptive wavelet methods. For simulations at moderate resolutions, such as 256^2, the adaptive wavelet methods cannot yet outperform the classical spectral methods. The majority of the computational time is spent in the vaguelette decomposition, and thus optimizing this part of the algorithm is a priority. The adaptive wavelet method is also a promising candidate for parallelization because all wavelet coefficients at a given scale may be calculated simultaneously, and only local memory sharing is required.

We conjecture that the density of vortices in a two-dimensional turbulent flow is essentially independent of Reynolds number because the coherent vortices inhibit the formation of new vortices in their vicinity [23]. If this is in fact the case, the wavelet method should be far more efficient at higher Reynolds numbers since the number of active modes scales with the number of vortices. The adaptive wavelet method is therefore proposed as a candidate for the DNS of high Reynolds number flows, rather than as a replacement for the pseudospectral methods currently used for moderate Reynolds number flows.

In a full turbulent flow there is more weak unorganized "background" structure than in our three vortex interaction. It is likely that this background will have to be modeled in some way in order to reproduce the physics of the flow correctly. The wavelet representation makes it easy to model the unorganized background and coherent parts of the flow as physically separate, but multiscale regions. This is not possible in a Fourier representation. The background could be modeled simply as a colored noise, calculated using a simple turbulence model such as k–ϵ [32], or a maximum entropy technique [36]. Another important issue in simulating statistically steady turbulence is the nature of the forcing used. We have recently proposed a more physical forcing based on the wavelet modes [40] which works naturally with the adaptive wavelet code examined here.

The extension of the adaptive wavelet method presented here to three-dimensional turbulent flows is attractive, but not completely straightforward. This is mostly due to the fact that in three dimensions the Navier–Stokes equations cannot be reduced to pseudoscalar equations, which increases the complexity of the problem. For example, we will require vector-valued wavelets which satisfy the incompressibility condition [24], [25], and a way of dealing efficiently with the large number of neighboring coefficients at each scale in three dimensions. Despite these difficulties, the compression properties of wavelets make them a promising technique for DNS of three-dimensional turbulence because the modulus of the vorticity field is mostly concentrated in low-dimensional coherent vortices: the vortex tubes [42], [43], [44]. However, it remains to be established whether the dynamics of three-dimensional turbulent flows are controlled by the coherent vortices.

In summary, we have found that the adaptive wavelet method produces highly accurate results with many fewer active modes than the classical pseudospectral method. The classical pseudospectral method is approaching a practical Reynolds number limit because it does not exploit the vortical structure of high Reynolds number flows, but the adaptive wavelet method promises greater efficiencies at high Reynolds numbers.

References

[1] W.T. Ashurst, A.R. Kerstein, R.M. Kerr, and C.H. Gibson, *Phys. Fluids* **30**(8), 2343 (1987).
[2] C. Basdevant, B. Legras, R. Sadourny and M. Béland, *J. Atmospheric Sci.* **38**, 2305 (1981).
[3] G.K. Batchelor, *Phys. Fluids* **12**, II-233 (1969).

[4] H. Bockhorn, J. Fröhlich, and K. Schneider. An Adaptive Two–Dimensional Wavelet–Vaguelette Algorithm for the Computation of Flame Balls, Preprint Institut für Chemische Technik, Universität Karlsruhe, (1996).

[5] G. Boffetta, A. Celani, A. Crisanti, and A. Vulpiani, *Phys. Fluids* **9**(3), 724–734 (1997).

[6] C. Canuto, M.Y. Hussaini, A. Quaternioni, and T. A. Zang, *Spectral Methods in Fluid Dynamics*, Springer-Verlag, Berlin, 1988.

[7] P. Charton and V. Perrier, *Comput. Appl. Math.* **15**, 139 (1996).

[8] I. Daubechies, *Ten Lectures on Wavelets*, SIAM, Philadelphia, 1992.

[9] P. Dimotakis, Turbulence, fractals and mixing in *Chaos, Turbulence and Mixing*, edited by E. Guyon, in press.

[10] D.G. Dritschel and D.W. Waugh, *Phys. Fluids* A **4**(8), 1737 (1992).

[11] M. Farge, *Ann. Rev. Fluid Mech.* **24**, 395 (1992).

[12] M. Farge, J.-F. Colonna, and M. Holschneider, Wavelet analysis of coherent structure in two-dimensional turbulent flows, in *Topological Fluid Mechanics*, edited by H.K. Moffatt and A. Tsinober, Cambridge University Press, Cambridge, 1990, p. 765.

[13] M. Farge, E. Goirand, Y. Meyer, F. Pascal, and M.V. Wickerhauser, *Fluid Dynamics Res.* **10**, 229 (1992).

[14] M. Farge, J. Guezennec, C.M. Ho, and C. Meneveau, Continuous wavelet analysis of coherent structures, in *Studying Turbulence Using Numerical Simulation Databases*, edited by P. Moin, W.C. Reynolds, and J. Kim, Center for Turbulence Research, Stanford, CA, 1990, p. 331.

[15] M. Farge, N. Kevlahan, V. Perrier, and E. Goirand, *Proc. IEEE* **84**, 639 (1996).

[16] M. Farge and G. Rabreau, *C. R. Acad. Sci. Paris Sér. II* **307**, 1479 (1988).

[17] J. Fröhlich and K. Schneider. *European J. Mech.* **B 13**, 439 (1994).

[18] J. Fröhlich and K. Schneider, *C. R. Math. Rep. Acad. Sci. Canada* **17**(6), 283 (1995).

[19] J. Fröhlich and K. Schneider, *Appl. Comput. Harm. Anal.* **3**, 393 (1996).

[20] J. Fröhlich and K. Schneider, Computation of Decaying Turbulence in an Adaptive Wavelet Basis, Preprint SC 96-11, Konrad-Zuse-Zentrum Berlin, 1996.

[21] J. Fröhlich and K. Schneider, *J. Comput. Phys.*, **130**, 174 (1997).

[22] J. Jiménez, A.A. Wray, P.G. Saffman, and R.S. Rogallo, *J. Fluid Mech.* **255**, 65 (1993).

[23] N.K.-R. Kevlahan and M. Farge, *J. Fluid Mech.* **346**, 49 (1997).

[24] P.G. Lemarié-Rieusset, *C. R. Acad. Sci. Paris Sér. I* **313**, 213 (1991).

[25] P.G. Lemarié-Rieusset, *Rev. Mat. Iberoamer.*, **8**, 221 (1992).

[26] J. Liandrat and P. Tchamitchian, *Resolution of the 1D Regularized Burgers Equation Using a Spatial Wavelet Approximation Algorithm and Numerical Results*, ICASE, Hampton, VA, 1990.

[27] J. McWilliams *J. Fluid Mech.* **219**, 361 (1989).

[28] C. Marchioro and M. Pulvirenti, *Mathematical Theory of Incompressible Nonviscous Fluids.* Springer-Verlag, Berlin, 1994, p. 139.

[29] M.V. Melander, N.J. Zabusky, and J.C. McWilliams, *J. Fluid Mech.* **195**, 303 (1988).

[30] C. Meneveau, *J. Fluid Mech.* **232**, 469 (1991).

[31] Y. Meyer, *Ondelettes et Opérateurs I/II*, Hermann, Paris, 1990.

[32] B. Mohammadi and O. Pironneau, *Analysis of the k-Epsilon Model*, Masson, Wiley, Paris, New York, 1993.

[33] J. von Neumann, Recent theories of turbulence (1949), in *Collected Works (1949–1963)*, Vol. 6, edited by A.H. Taub, Pergamon Press, Oxford, 1963, p. 437.

[34] G.S. Patterson and S.A. Orszag, *Phys. Fluids* **14**, 2538 (1971).

[35] V. Perrier and C. Basdevant, *Rech. Aérospat.*, **3**, 53 (1989).

[36] R. Robert and J. Sommeria, *J. Fluid Mech.* **229**, 291 (1991).

[37] R.S. Rogallo, NASA Tech. Memo. 73203 (1977).

[38] R.S. Rogallo, NASA Tech. Memo. 81315 (1981).

[39] R.S. Rogallo and P. Moin, *Ann. Rev. Fluid Mech.* **16**, 99 (1984).

[40] K. Schneider and M. Farge *C. R. Acad. Sci. Paris Sér. II* **325** IIb, 263–270 (1997).

[41] A. Siegel, J.B. Weiss, *Phys. Fluids*, **9**(7), 1988–1999 (1997).

[42] A. Vincent and M. Meneguzzi, *J. Fluid Mech.* **225**, 1 (1991).

[43] A. Vincent and M. Meneguzzi, *J. Fluid Mech.* **258**, 245 (1994).

[44] M. V. Wickerhauser, M. Farge, E. Goirand, E. Wesfreid, and E. Cubillo, Efficiency comparison of wavelet packet and adapted local cosine bases for compression of a two-dimensional turbulent field, in *Wavelets: Theory, Algorithms and Applications*, edited by C.K. Chui, L. Montefusco, and L. Puccio, Academic Press, New York, 1994, p. 509.